

Technique for normalizing intensity histograms of images when the approximate size of the target is known: Detection of feces on apples using fluorescence imaging

Alan M. Lefcouth*, Moon S. Kim

*USDA Agricultural Research Service, Instrumentation and Sensing Laboratory, Henry A. Wallace Beltsville
Agricultural Research Center, Beltsville, MD, USA*

Received 20 January 2005; received in revised form 30 September 2005; accepted 6 October 2005

Abstract

A challenge in machine vision is to develop algorithms for detecting a substance with an amorphous shape when measured responses of both the substance and the underlying target have similar characteristics. The challenge is exacerbated when responses for targets are highly variable both across and within discrete target units. An example of this problem is the detection of fecal contamination on apples. Feces on apples can be detected using differential fluorescence responses of contaminated and uncontaminated apple surfaces to UV excitation. However, responses of both feces and apples are due to the presence of chlorophyll-related compounds, and the response of apples varies within and between apples due to natural variation in the distribution of these compounds. We present a technique for normalizing the variability of intensity responses among targets based on a priori knowledge of the image dimensions and the approximate target size. Using this information, a linear equation is derived based on the approximate median intensities of the background and of the target. The median intensities are estimated by calculating a cumulative intensity histogram and using a priori estimates of the percentage of the area in the image occupied by the background and by a generic target. The image is scaled for uniform intensity power using this linear transformation. The benefits of using this technique are demonstrated using hyperspectral fluorescence responses to UV excitation of 48 Golden Delicious and 48 Red Delicious apples artificially contaminated with dilutions of cow feces. Results show that the uniform power transformation normalizes the intensity distributions of apple images and increases the contrast between contaminated and uncontaminated areas on apple surfaces; the coefficients of variation for the average intensities of uncontaminated apple surfaces at 668 nm for Golden and Red Delicious apples were reduced from 39 and 55%, respectively, to 5% for both varieties.

Published by Elsevier B.V.

Keywords: Fluorescence; Hyperspectral imaging; Imaging; Fecal contamination; Methodology

1. Introduction

There is an increasing use of imaging for automated quality control of agricultural products (Chen et al., 2002). A common problem is the detection of a foreign contaminant on a known target. Often the contamination site has an amorphous shape, e.g., contamination due to splatter, which prevents utilization of shape-based detection algorithms. The challenge of developing algorithms to detect amorphous contamination sites is exacerbated when intensities

* Corresponding author. Tel.: +1 301 504 8450; fax: +1 301 504 9466.
E-mail address: alefcour@anri.barc.usda.gov (A.M. Lefcouth).

of target objects in images are highly variable both across and within individual objects. The detection of fecal contamination on apples is a good example of this problem. The authors have demonstrated that, with appropriate excitation, feces from many species fluoresce in the red band due to the presence of chlorophyll-related compounds (Kim et al., 2003; Lefcourt et al., 2003). However, detection of feces on apples is complicated by the fact that apples contain chlorophyll-related compounds and fluorescence responses of individual apples are highly variable (Kim et al., 2002). To address this problem, a technique was developed to normalize the intensity histograms of images.

Detection of fecal contamination on apples is a critical health safety issue as feces can be the source of a number of human pathogens (Armstrong et al., 1996; Blackburn and McClure, 2002; Hui, 2001; Mead et al., 1999). The FDA has solicited development of systems to detect contaminated apples (FDA, 2001). In this regard, the authors have developed and refined algorithms for the automated detection of feces on apples based on differential fluorescence responses of contaminated and uncontaminated apple surfaces (Lefcourt et al., 2003, 2005a,b,c). During the refinement process, it was found that use of a uniform power transformation enhanced detection of feces on apples (Lefcourt et al., 2005b,c), and that a uniform power transformation based on the median intensity of individual apple surfaces performed better than an analogous transformation based on near maximal intensity (Lefcourt et al., 2005c).

The purpose of this study is to elucidate the properties and benefits of this technique for normalizing the intensity histograms of images based on a priori knowledge of the dimensions of an image and the approximate size of a target. Apples artificially contaminated with dairy feces were used for testing as the highly variable fluorescence response of apples to UV excitation provided the impetus for developing this technique. The use of hyperspectral images in the visible range, from 443 to 729 nm, allows examination of the effects of this uniform power transformation on average spectra of untreated apple surfaces and of areas of fecal contamination.

2. Methods

Golden Delicious and Red Delicious apples were artificially contaminated with titrations of dairy feces and subsequently scanned using a hyperspectral imaging system for fluorescence responses to UV-A excitation. Two image sets were constructed, with the difference that in the second image set individual apples at each wavelength were subject to a novel uniform power transformation (below). Intensity and average spectral responses of control and contamination sites were compared for the normal and the transformed image sets by apple variety.

2.1. Apples and feces application

The Red Delicious and Golden Delicious apples were from crates of tree-run apples at the Rice Fruit Co. (Gardners, PA) and were stored at 3 °C. Apples for treatment were selected randomly with the restrictions that apples were undamaged and free of rot. Feces were applied to 48 apples of each type.

Fresh cow feces were collected at the Beltsville Agricultural Research Center dairy. The feces was immediately diluted and applied to the apples. Dry-matter content of the feces ($14.8 \pm 0.2\%$) was determined by drying three samples to a constant weight in a 95 °C oven. The fresh feces were serially diluted 1:2, 1:20, and 1:200 (w/w) with deionized water. A single 30 μ l drop of each of the three dilutions was applied to the cheek surface of individual apples using a pipette with one drop per quadrant; the fourth, control, quadrant was not treated (Fig. 1). To accommodate particulates in the dilutions, about 2 mm was cut-off of the end of the pipette tip using a razor blade. Treated apples were stored at 3 °C, and were allowed to warm to room temperature for approximately 30 min prior to imaging.

2.2. Hyperspectral imaging system

The imaging hardware consists of a camera, a prism-grating system, and a zoom lens mounted over a single-axis transition table along with UV-A illumination sources. Hyperspectral data sets are constructed from a series of images taken as an object is incrementally moved under the camera. For each image, the imaging area is a line across the object perpendicular to the direction of movement; the prism-grating system decomposes each spatial pixel along the imaging line into its spectral components. The camera (Model DV465, Andor Technology) utilizes an electron-multiplying CCD with 560 pixels in the spatial and 288 pixels in the spectral dimensions, and has 16-bit resolution. The prism-grating system (ImSpector V9, Specim) has a spectral range from 430 to 900 nm, and uses a slit-width of 50 μ m to produce a

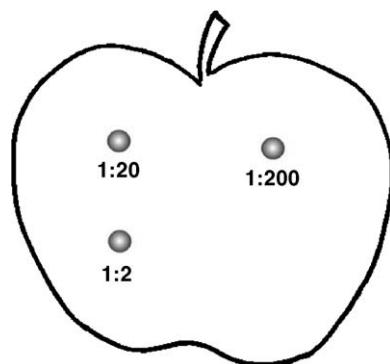


Fig. 1. Application sites for 30 μ l of 1:2, 1:20, and 1:200 serial dilutions of dairy feces. The order of the applications followed a clockwise rotation based on concentration. The initial quadrant for application of the 1:2 dilution was incremented one quadrant clockwise every fourth apple.

spectral resolution of about 4.5 nm. The lens (2/3"; S6X11, Rainbow) allows focal lengths from 11.5 to 69 mm. The transition table (B-Slide, Velmex) is about 61 cm in the direction of movement by 36 cm, and is controlled using a stepper motor with a resolution better than 0.01 mm. For illumination, two 30° UV-A light sources (Model XX-15A, Spectraline) are positioned 28 cm above the table and on each side of the imaging line at an angle of 18° relative to the vertical axis; output is restricted to between 300 and 400 nm using band-pass filters (UG-1, Schott Glass).

2.2.1. System operation

A program written in Visual Basic Version 6® (Microsoft) is used to control the transition table and acquire images, and for preliminary data analyses. The transition table is controlled using a serial interface and ASCII commands. The camera is controlled via a dynamically linked library (DLL) from a software development kit provided by the camera manufacturer (Andor Technology). For this study, a pixel area of about 0.5 mm² was accomplished by moving the transition table in 0.5 mm increments and adjusting the zoom lens appropriately. Fluorescence images were taken in the dark with an exposure time of 0.3 ms, a gain of 255, and the detector maintained at −38 °C using three-stage Peltier cooling. The net acquisition time for individual images was essentially the sum of the exposure time and the time used to move the table to the next imaging position. As the A/D conversion rate was not a limiting factor, only one of the two existing A/D converters was used to eliminate potential bias. After completion of an individual scan sequence, data were converted to a single hyperspectral image file using the ENVI® (Research Systems, Inc.) file format.

2.2.2. System calibration

The spectral response of the system was determined using known light sources as described by Kim et al. (2001). For fluorescence measurements, the spectral dimension was binned by 2, and only 65 of the resulting 144 channels were used. Wavelengths for these 65 channels ranged from 443 to 729 nm with a separation between adjacent channels of about 4.4 nm. Tests indicated that it was not necessary to correct for individual pixel responsivity. However, a curvilinear response due to illumination was identified along the imaging axis. The curvilinear response resulted from the use of light sources that are of the same dimension as the width of the translation table; hence, the outer extremes of the imaging area receive progressively less illumination. As the response was essentially flat in the middle two-thirds of the imaging axis, imaging for this study was limited to this area (~24 cm). To meet this dimensional constraint, two parallel rows of six rubber cups were used to hold apples for imaging. Resulting images were corrected only for dark currents.

2.3. Data analyses

The hyperspectral images were analyzed using ENVI® (Research Systems, Inc.) and a series of programs written in Visual Basic Version 6® (Microsoft). All Basic programs relied on a library of functions developed in-house that allowed a range of image manipulations (e.g., brightness, contrast, normalization, exponential scaling, and functional combinations of images including ratios), filters (e.g., spatial, geometric, morphological, edge, and threshold; Weeks, 1996), and graphic displays such as false color images and histograms.

2.3.1. Creation of masks

One program allowed the semi-automated creation of rectangular masks. For this study, square masks of 187 by 187 pixels were used to locate individual apples within raw images. Given that the physical location of apples was the same for all wavelengths, it was possible to use these masks to create a single large image file for each variety of apples with six apples per column by eight apples per row at each wavelength. Similarly, square masks of 15 by 15 pixels were used to locate contamination sites and an untreated, control, area in the untreated control quadrant for each apple. The locations of the 15 by 15 pixel masks were automatically indexed to the location of individual apples in the single large image files.

Masks that encompassed the surface area of individual apples were created using binary thresholds. Morphological filtering was used to smooth these mask and to remove noise speckles. Subsequently, the 15 by 15 pixel areas corresponding to contamination sites were excluded from the masks. Thus, these masks represent the uncontaminated surface areas of individual apples. A single set of apple masks was created for each apple variety.

2.3.2. Uniform power transformation

The uniform power transformation is a linear transform of image intensities. The x -axis coordinates of the two points used to determine the equation of the line are based on the cumulative histogram of an individual image. One coordinate is the intensity value of the 75% level of the histogram ($C_{75\%}$); the second is the value at 5% ($C_{5\%}$). With the imaging system specifications used in this study, apples occupied about 50% of the imaging area. Thus, the $C_{75\%}$ intensity value corresponds to the median intensity of the surface of a generic apple. The dark background occupied the other approximate 50% of imaging areas. As the background intensity showed little variation, the $C_{5\%}$ intensity value was chosen to represent the median background intensity instead of the $C_{25\%}$ value. This substitution addressed the possibility that a very large apple might encompass more than 75% of the imaging area. The y -coordinates of the two points used to determine the line were 65 and 20, respectively. Thus, images of individual apples were adjusted for uniform intensity power using the following linear equation to map measured pixel intensities (I_{in}) of an individual image to corresponding output intensities (I_{out}):

$$I_{out} = \text{Slope} \times I_{in} + \text{Intercept}$$

$$\text{If } I_{out} > 1023 \text{ then } I_{out} = 1023$$

$$\text{If } I_{out} < 0 \text{ then } I_{out} = 0$$

where

$$\text{Slope} = \frac{65 - 20}{C_{75\%} - C_{5\%}}$$

$$\text{Intercept} = 65 - \text{Slope} \times C_{75\%}$$

Resulting intensity values (I_{out}) less than 0 or greater than 1023 were set to 0 or 1023, respectively.

2.3.3. Transformations used for comparisons

To allow comparison of the benefits of the uniform power transformation, raw images of apples were subjected to some common transformations. Ratio images were created by dividing pixel intensity values at one wavelength by the corresponding intensity values at a second wavelength, multiplying the quotient by 1000, and then adding 50. Raw images were linearly scaled to intensities of 0–255. Finally, individual apple images were scaled using 1% histogram stretching, i.e., each image was scaled to 0–255 using the corresponding 1 and 99% thresholds of the cumulative histogram as end-points.

As software for personnel computers generally will only display gray-scale images with 8-bit resolution, images for display were scaled to 8-bit resolution using 1% histogram stretching. Transformation of display images was done only to allow visualization of images.

2.3.4. Spectra

Spectra were calculated by averaging intensities within the appropriate 15 by 15 pixel masks (above). These values were then averaged across the 48 apples of each type to yield average spectra. Average spectra were calculated for raw and transformed image sets. To elucidate the contrast between treatment and control spectra at a given wavelength, contrast ratios were calculated as the ratio of the treatment to the control spectral values at each wavelength.

2.3.5. Measures related to variation of intensities of apple surfaces

The apple masks were used to determine statistics for uncontaminated surface areas of individual apples by wavelength for raw and transformed image sets. To examine inter-apple variability, the coefficients of variation (CV) of the average intensity of individual apples were calculated for selected wavelengths within image sets. To examine intra-apple variability, coefficients of variation were calculated for individual apples and averaged.

Variability can be reduced by removing information content from images. As a measure of information content relative to detection of contamination sites, relative response differentials were calculated for each dilution of applied feces for selected wavelengths within image sets. To calculate the measures, the mean of average intensities of uncontaminated apples surfaces was determined for the selected image set and wavelength ($n=48$). For each individual contamination site in the selected image set, the average intensity within the 5 by 5 pixel area in the center of the 15 by 15 pixel contamination mask were determined. The mean intensity for uncontaminated surface areas was subtracted from this contamination site average, and the result was divided by the same overall mean. Measures were averaged by level of contamination. Essentially, this measure represents the average differential response at a given wavelength due to contamination scaled to the mean intensity of the corresponding uncontaminated surfaces.

3. Results and discussion

There are a number of existing methods for transforming images based on some function of the corresponding cumulative intensity histogram, e.g., histogram stretching or thresholding. Generally, these transformations use end-

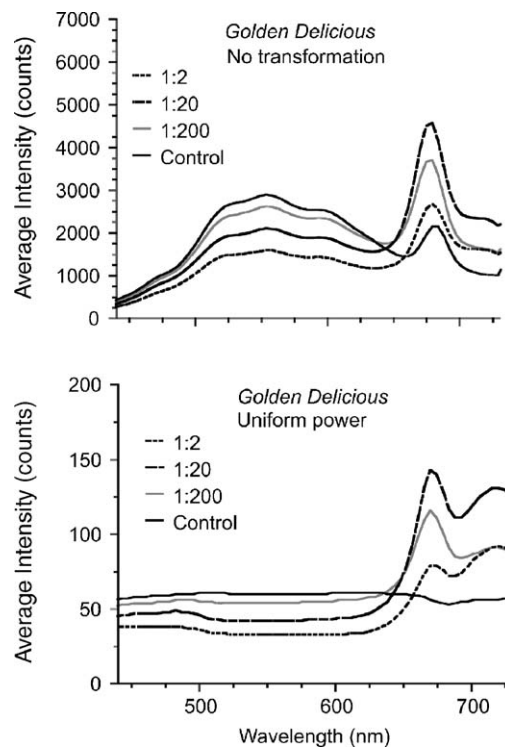


Fig. 2. Average spectral responses of areas treated with dilutions of cow feces and of untreated, control, areas for 48 Golden Delicious apples. The top graph shows responses for untransformed images. The bottom graph shows responses when images of individual apples were subject to the uniform power transformation at each wavelength.

points for re-mapping intensity distributions, and any intensity values outside the end-points are truncated. In contrast, the uniform power transformation is a function of two points within the cumulative intensity histogram and the end-point (truncation) values can be selected independent of the points used to create the transform equation. In addition, end-point based transformations are inappropriate when an image component of interest is heavily represented at either extreme of the corresponding cumulative intensity histogram; i.e., truncation would disproportionately reduce the information content relative to the component of interest. Problems can also result when the intensity value of an end-point has the potential to vary dramatically. An example of this problem situation relates to the question of detecting fecal contamination. Intensity values at the upper end of the cumulative histogram for images with contaminated targets will generally be much higher than similar values for images of uncontaminated targets. If images were scaled to corresponding near maximal intensity values, the process would accentuate any naturally bright spot found in an image of an uncontaminated target, which would likely result in the bright spot being detected as a false positive. On a practical basis, empirical tests of the uniform power transformation demonstrated that detection of feces on apples was improved when the transformation was based on the approximate median intensity of apples rather than on a near maximal intensity (Lefcourt et al., 2005c).

Selection of parameters used for defining the uniform power transform involves consideration of a number of factors. There is considerable leeway in selecting the lower x -coordinate used to define the transformation. Variation in the intensities of background pixels is primarily a function of the noise level of the instrumentation. The cumulative percentage used for defining the uniform transformation need only exceed the noise level and be less than any percentage that might include responses from an unusually large target. Given this lack of sensitivity, it would be feasible to replace this lower coordinate with a fixed value. However, there are advantages for using a dynamic value. A dynamic value will allow compensation for any change in the sensitivity of the instrumentation, e.g., if the camera CCD was not temperature-controlled and ambient temperature varies. Furthermore, there is essentially no cost to using a dynamic value, as the cumulative histogram has to be calculated in any case.

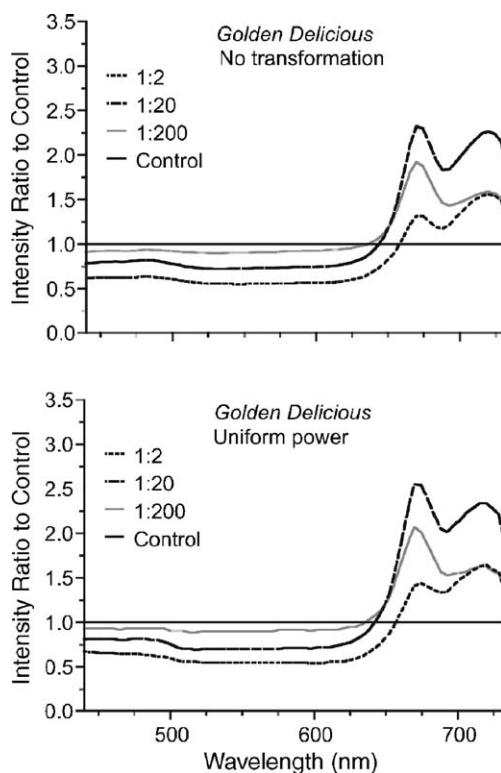


Fig. 3. The ratio of spectral responses for contaminated areas from Fig. 2 to the appropriate control spectra by wavelength. Note that the relative amplitudes of the resulting spectra in the red region were greater when individual apple images were subjected to the uniform power transformation.

Table 1

Maximum intensity ratios of treated to control areas in the red region of the spectrum by apple variety and applied feces dilution, with and without use of the uniform power transformation

Apple variety	Transformation	Maximum intensity ratios ^a		
		Applied feces dilution		
		1:2	1:20	1:200
Golden Delicious	None	1.32	2.32	1.92
	Uniform power	1.44	2.55	2.07
Red Delicious	None	1.40	2.68	2.20
	Uniform power	1.61	3.17	2.43

^a Maximum ratio of a treated to the corresponding control spectral value at a single wavelength in the region from 650 to 700 nm.

The upper x -coordinate for defining the uniform power transformation was selected to be the 75% intensity level of the cumulative histogram; as apples accounted for about 50% of the image area on average, this value corresponds to the median intensity of a generic apple. This selection carries the implicit assumption that less than 25% of the area of any image will represent contamination. It is theoretically possible to use a variable upper percentage based on some measure of the actual area in the image occupied by a particular apple, the distribution of the cumulative histogram, or some combination of both. The difficulty is defining an algorithm for selecting a threshold that actually would improve detection. For apples, a particular problem is the range of variability of fluorescence responses across the surface of individual apples. For example, apple surfaces exposed to sunlight have lower chlorophyll concentrations compared to surfaces of the same apple that were shaded during growth (Kim et al., 2002). The resulting differences in measured responses exceed the error associated with using a fixed percentage value of the cumulative histogram to define the transformation. For situations where intra-target variability is low, a functionally derived upper threshold might warrant consideration.

Selection of the y -coordinates for the two points used to define the uniform power transformation involves practical and functional considerations. A practical consideration is the ability to easily display transformed images on a computer

Table 2

Measures of variability and relative response differential following application of selected image transformations ($n = 48$)

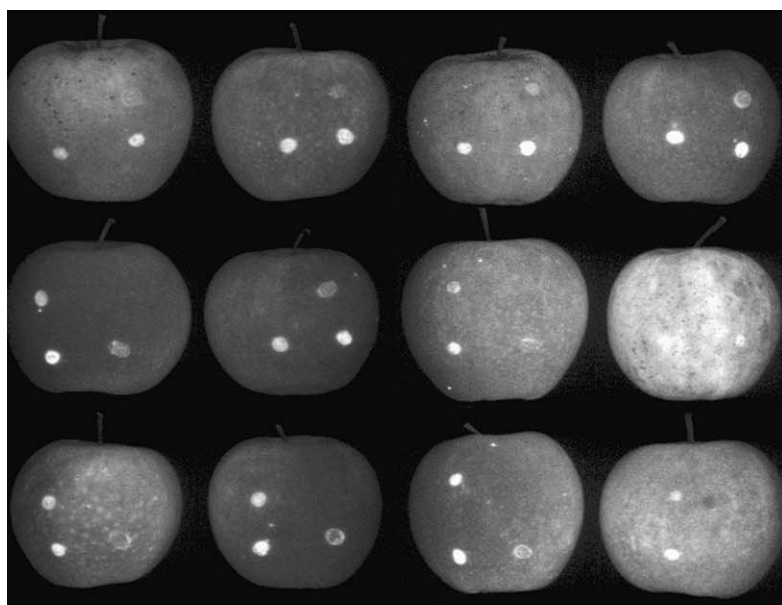
Apple variety	Transformation	Wavelength (nm)	Measures of variability for uncontaminated apple surfaces ^a		Measures of relative response differential ^b		
			Inter-apple CV ^c	Average intra-apple CV	Applied feces dilution		
					1:2	1:20	1:200
Golden Delicious	None	668	0.39	0.32	0.55	1.74	1.27
	Uniform power	668	0.05	0.32	0.66	1.99	1.42
	Ratio	668/482	0.35	0.32	1.32	1.41	1.03
	Linear 0–255	668	0.42	0.34	0.54	1.43	1.16
	1% histogram stretch	668	0.42	0.32	0.43	1.18	0.95
	None	482	0.41	0.25			
Red Delicious	Uniform power	482	0.05	0.25			
	None	668	0.55	0.34	0.47	1.88	1.40
	Uniform power	668	0.05	0.32	0.77	2.51	1.68
	Ratio	668/482	0.35	0.28	1.20	1.28	1.26
	Linear 0–255	668	0.59	0.36	0.49	1.71	1.33
	1% histogram stretch	668	0.59	0.35	0.48	1.76	1.31
	None	482	0.33	0.32			
	Uniform power	482	0.07	0.27			

^a Entire apple surfaces were used for calculations with the exception of areas marked by contamination masks.

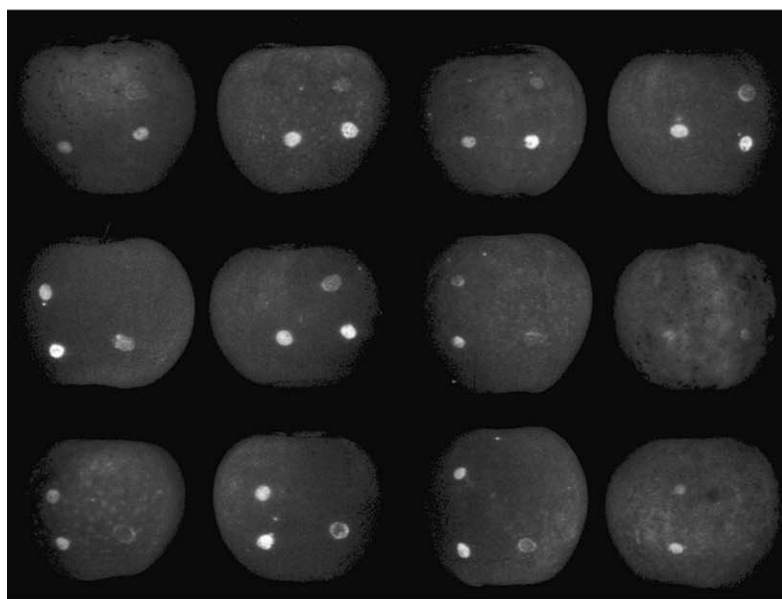
^b Average of mean intensities of individual contamination sites minus overall mean intensity of corresponding uncontaminated surfaces divided by the same overall mean.

^c Coefficient of variation.

monitor. Most computer software for displaying images is based on 24-bit color images with 8-bits each for red, green, and blue. Gray-scale images are created by replicating gray-scale values across the three colors; false color images are created by selectively mapping the 8-bit gray-scale values to the three-color space. Thus, gray-scale images for display must be 8-bit, which can most readily be accomplished as part of the transformation process or by truncation of images to 8-bits. For this study, the principle functional consideration was to retain the dynamic range of fluorescent responses in images. The y-coordinate value of 65, which corresponds to the 75% of the cumulative intensity histogram, guarantees that the target will be visible in the transformed image, even if the transformed image is truncated to 8-bits for display. The y-coordinate value of 20, which corresponds to the black (background) pixel intensity, results in the



(a) Golden Delicious - No transformation



(b) Golden Delicious - Uniform power

Fig. 4. Representative portion of the large image for Golden Delicious apples at 674 nm. Note the muted, consistent, intensity of the apples in the bottom image where individual apples were subjected to the uniform power transformation.

compression of non-critical target information while allowing for reasonable contrast when the truncated image is displayed. This compression, along with the use of 10-bits to represent the transformed image, permits retention of the dynamic range of the intensity responses of contamination sites.

The spectral responses of contaminated and untreated areas on Golden Delicious apples are shown in Fig. 2. As was previously found, there was no direct relation between the concentration of feces applied and the corresponding fluorescence response (Kim et al., 2003; Lefcourt et al., 2003, 2005b). The measured responses for treated areas include contributions from the feces and from the underlying apple surface. Thick applications of feces, such as the 1:2 dilution, impede both the excitation and the response of the underlying surfaces, and high concentrations of fluorophors in the feces can reabsorb emissions from apple surfaces. In contrast, measured responses for thin applications, such as the 1:20 dilutions, which were visually transparent, are probably a summation of the responses of the feces and the underlying apple surfaces. In addition, the authors found that application and then removal of feces after a period of hours results in a detectable fluorescence response in the areas formerly covered by feces (Lefcourt et al., 2003, 2005a). This fluorescence response probably augments measured responses for thin feces applications. Prior studies demonstrated that the magnitude of fluorescent responses of feces peaked in the red region of the spectrum (Kim et al., 2002, 2003), and that this region could be used to detect feces on apples (Kim et al., 2002; Lefcourt et al., 2003). Comparison of spectra for normal and transformed images (Fig. 2) show that the uniform power transformation highlights the regions of the spectrum, including the red region, where the spectra for contaminated areas show the greatest differences from spectra for untreated areas.

A common method for examining the contrast between treatment and control spectra is to calculate the ratio of the treatment to the control spectral values at each wavelength (Fig. 3). For the Golden Delicious apples, taking these ratios reduced the apparent differences between sets of spectra for normal and transformed images. Shapes for both sets of spectra were similar; however, the uniform power transformation increased the relative amplitudes of the spectra in the

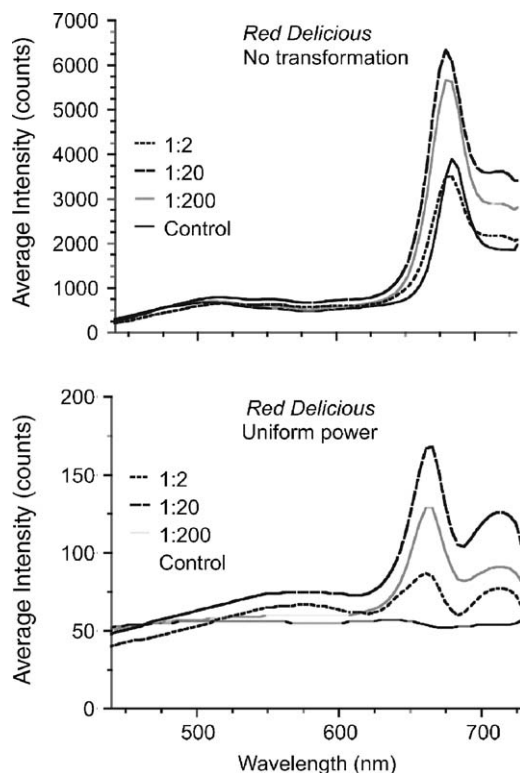


Fig. 5. Average spectral responses of areas treated with dilutions of cow feces and of untreated, control, areas for 48 Red Delicious apples. The top graph shows responses for untransformed images. The bottom graph shows responses when images of individual apples were subject to the uniform power transformation at each wavelength.

red region for contaminated areas (Table 1). These increased amplitudes can be interpreted as an increase in the contrast between contaminated and untreated apple surfaces. Examination of actual images at the peak wavelength confirm that the uniform power transformation mutes the differences in natural fluorescence responses among different apples, and increases the relative contrast between contaminated and untreated surface areas (Fig. 4). Essentially identical results were obtained for Red Delicious apples (Figs. 5–7; Table 1).

The effects of the uniform power transformation on the variability of intensity across composite images of 12 Golden Delicious or 12 Red Delicious apples are apparent in the histograms shown in Fig. 8. In the normal histograms for both varieties, there are secondary peaks starting at intensities just over 50 due to greener apples that appear brighter in Figs. 4 and 7. The transformation normalized and reduced the spread of the intensity histograms, and in so doing eliminated these secondary peaks. In the histograms for transformed images, pixel intensities of contaminated areas account for essentially all of the tails of the histograms.

The variability of inter- and intra-target intensities can be compared using coefficients of variation. Table 2 shows examples of intensity variability of Golden and Red Delicious image sets at 668 and 482 nm. The 668 nm represents the peak, or near peak, wavelength in the spectra of the fluorescence response of feces. The 482 nm wavelength was selected as ratios created by dividing a red region image by a blue region image have been demonstrated to enhance detection of thick applications of feces applied to apples (Kim et al., 2002; Lefcourt et al., 2003). Ratios enhance detection by reducing intensity variability and, more importantly, by enhancing the contrast between contaminated and uncontaminated areas on an apple surface. The increased contrast results because thick contamination sites are brighter than surrounding areas in the red-region images, and darker than the surrounding areas in corresponding blue-region images. The uniform power transformation greatly reduced inter-apple variability compared to raw or 668/482 ratio image sets, and images transformed using 1% histogram stretching or linear scaling to 8-bits. Some reduction in inter-apple variability was achieved using ratios for Red Delicious apples. Average intra-apple variability was wavelength dependent, but varied little by transformation.

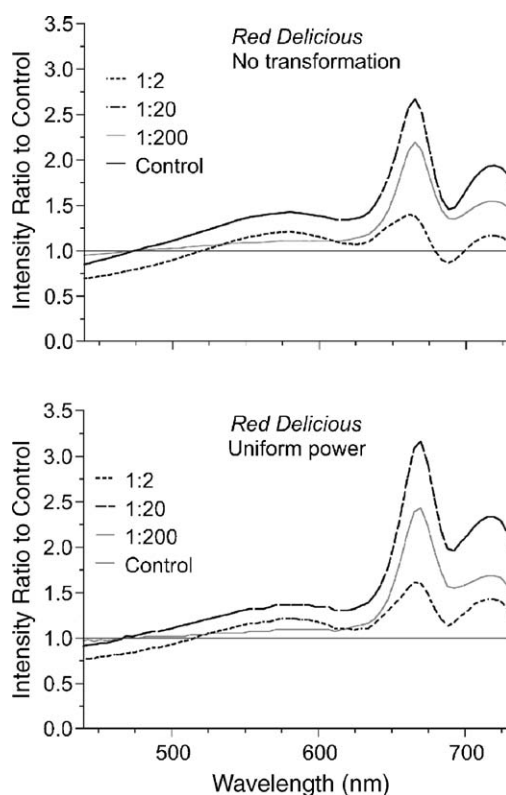
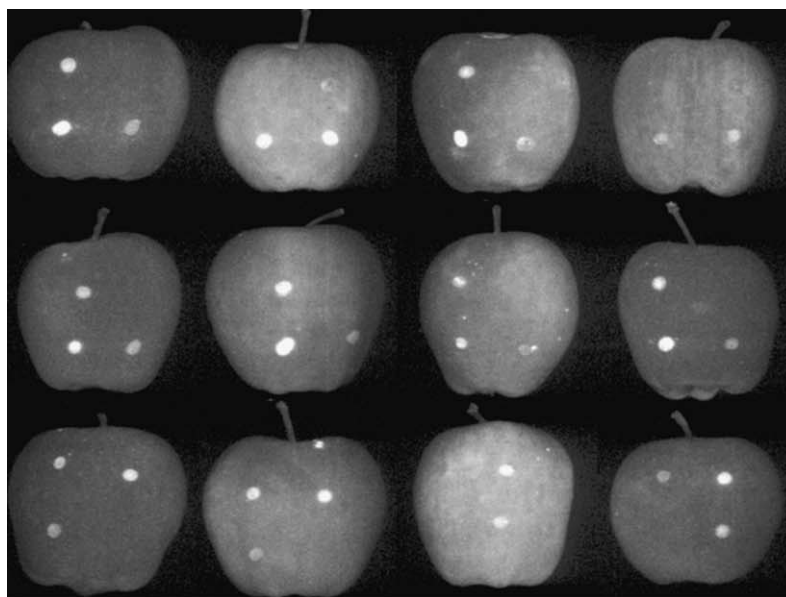
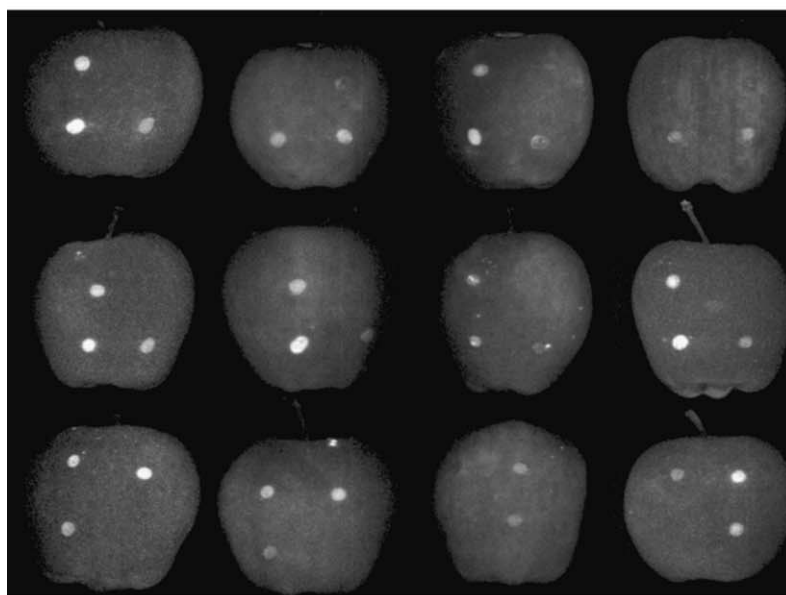


Fig. 6. The ratio of spectral responses for contaminated areas from Fig. 5 to the appropriate control spectra by wavelength. Note that the relative amplitudes of the resulting spectra in the red region were greater when individual apple images were subjected to the uniform power transformation.

To test if the uniform power transformation preserves or enhances information content relative to detection of contamination sites, relative response differentials were calculated for the three levels of contamination. This measure represents the average differential response due to contamination scaled to the mean intensity of corresponding uncontaminated apple surfaces. The measures, by level of contamination, were highest following use of the uniform power transformation with one exception (Table 2). Measures for ratio images were highest for 1:2 dilutions of applied feces; measures for the uniform power images were second highest. This finding is consistent with results from a prior study that demonstrated that ratio images were useful for detecting 1:2 dilutions of feces on Red Delicious apples (Lefcourt et al., 2003). In any case, the performance of the uniform power transformation for the 1:2 dilution may be adequate for development of commercial systems to detect contaminated apples.



(a) Red Delicious - No transformation



(b) Red Delicious - Uniform power

Fig. 7. Representative portion of the large image for Red Delicious apples at 665 nm. Note the muted, consistent, intensity of the apples in the bottom image where individual apples were subjected to the uniform power transformation.

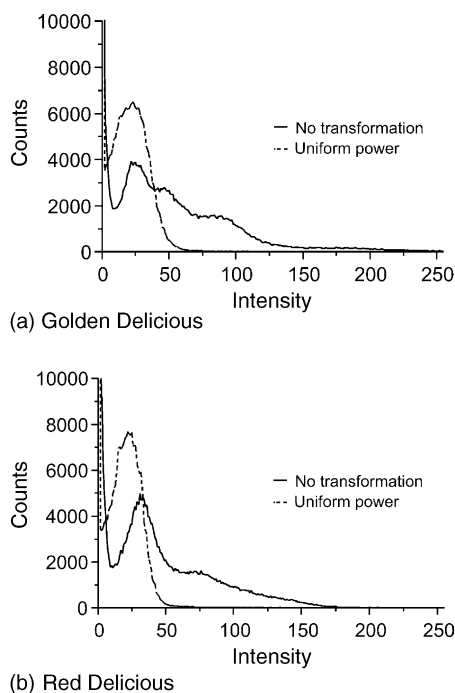


Fig. 8. The intensity histograms for the images of the 12 Golden Delicious apples in Fig. 4 and the Red Delicious apples in Fig. 7 show that, when individual apples were subjected to the uniform power transformation, the result is a single, uniform, distribution when pixels with 0 intensity are ignored. Note that the lower variability of intensities for Red Delicious compared to Golden Delicious apples results in a transformed intensity histogram that is relatively taller and narrower compared to the transformed intensity histogram for Golden Delicious apples.

The uniform power transformation is very simple and fast, and can greatly reduce the intensity variability among images of similar-sized objects. This reduction in variability can enhance detectability when discrimination is a function of intensity, e.g., red band response of apple and feces. A multispectral approach for detection of contamination such as fecal has been suggested for on-line inspection systems. One of the reason for using multispectral imaging concerns problems related to variability of target intensities. If a single wavelength system using the uniform power transformation can be used to instead of a multispectral imaging system, considerable cost savings can be achieved. Results indicate that this may be the case for detection of feces on apples.

4. Conclusion

It is possible to utilize a priori knowledge of an image size and the approximate size of the target to normalize intensity histograms by transforming images using a linear equation determined by the median intensity of the background and the median intensity of the target. Application of such a uniform power transformation to fluorescence images of apples artificially contaminated with feces essentially eliminated the variability among images due to natural differences in fluorescence responses to UV excitation among apples, and improved the contrast between contaminated and untreated apple surfaces. This normalization and increased contrast can be used to enhance the detection of contaminated areas on the surface of apples.

References

- Armstrong, G.L., Hollingsworth, J., Morris Jr., J.G., 1996. Emerging foodborne pathogens: *Escherichia coli* O157:H7 as a model of entry of a new pathogen into the food supply of the developed world. *Epidemiol. Rev.* 18, 29–51.
- Blackburn, C.W., McClure, P.J. (Eds.), 2002. *Foodborne Pathogens: Hazards, Risk Analysis, and Control*. CRC Press, Cambridge.
- Chen, Y.R., Chao, K., Kim, M.S., 2002. Machine vision technology for agricultural applications. *Comput. Electron. Agricult.* 33, 173–191.
- Food and Drug Administration (FDA), 2001. Hazard analysis and critical control point (HAACP). Procedures for the safe and sanitary processing and importing of juices. *Federal Registry* 66, 6137–6202.

- Hui, Y.H. (Ed.), 2001. *Foodborne Disease Handbook*. Marcel Dekker, New York.
- Kim, M.S., Chen, Y.R., Mehl, P.M., 2001. Hyperspectral reflectance and fluorescence imaging system for food quality and safety. *Trans. ASAE* 44, 721–729.
- Kim, M.S., Lefcourt, A.M., Chen, Y.R., Kim, I., Chao, K., Chan, D., 2002. Multispectral detection of fecal contamination on apples based on hyperspectral imagery. II. Application of fluorescence imaging. *Trans. ASAE* 45, 2027–2038.
- Kim, M.S., Lefcourt, A.M., Chen, Y.R., 2003. Optimal fluorescence excitation and emission bands for detection of fecal contamination. *J. Food Protect.* 66, 1198–1207.
- Lefcourt, A.M., Kim, M.S., Chen, Y.R., 2003. Automated detection of fecal contamination of apples by multispectral laser-induced fluorescence imaging. *Appl. Opt.* 42, 1–9.
- Lefcourt, A.M., Kim, M.S., Chen, Y.R., 2005a. A transportable fluorescence imaging system for detecting fecal contaminants. *Comput. Electron. Agricult.* 48, 63–74.
- Lefcourt, A.M., Kim, M.S., Chen, Y.R., 2005b. Detection of fecal contamination on apples with nanosecond-scale time-resolved imaging of laser-induced fluorescence. *Appl. Opt.* 44, 1160–1170.
- Lefcourt, A.M., Kim, M.S., Chen, Y.R. 2005c. Detection of fecal contamination in apple calyx by multispectral laser-induced fluorescence. *Trans. ASAE* 48, 1587–1593.
- Mead, P.S., Slutsker, L., Dietz, V., McCaig, L.F., Bresee, J.S., Shapiro, C., Griffin, P.M., Tauxe, R.V., 1999. Food-related illness and death in the United States. *Emerg. Infect. Dis.* 5, 607–625.
- Weeks Jr., A.R., 1996. *Fundamentals of Electronic Image Processing*. SPIE Optical Engineering Press, Bellington, Washington.